Copyright Warning & Restrictions

The copyright law of the United States (Title 17, United States Code) governs the making of photocopies or other reproductions of copyrighted material.

Under certain conditions specified in the law, libraries and archives are authorized to furnish a photocopy or other reproduction. One of these specified conditions is that the photocopy or reproduction is not to be "used for any purpose other than private study, scholarship, or research." If a, user makes a request for, or later uses, a photocopy or reproduction for purposes in excess of "fair use" that user may be liable for copyright infringement,

This institution reserves the right to refuse to accept a copying order if, in its judgment, fulfillment of the order would involve violation of copyright law.

Please Note: The author retains the copyright while the New Jersey Institute of Technology reserves the right to distribute this thesis or dissertation

Printing note: If you do not wish to print this page, then select "Pages from: first page # to: last page #" on the print dialog screen

ABSTRACT

DISPERSION AND DISSOLUTION KINETICS OF API PARTICLES IN PHARMACEUTICAL HOT MELT EXTRUSION

by
Wang Zhan

Pharmaceutical Hot Melt Extrusion (HME) is essentially a special case of polymer compounding. The elementary steps involved in traditional plastics melt processing are handling of particulates, melting, dispersive and distributive mixing, devolatilization and stripping, and finally pressurization and pumping. However, for pharmaceutical HME, the dissolution of the API (Active Pharmaceutical Ingredient) is an additional and very important elementary step, along with the melting of the polymeric excipient that precedes it, and mixing which accelerates the dissolution process. A major concern in pharmaceutical HME is the thermal degradation of the API. To avoid overexposure of API to heat while ensuring complete dissolution of the API in the production of solid solution, the dissolution kinetics of the API must be known. This work employs a non-dissolving, surrogate material in an attempt to deconvolute the phenomena of distribution, dispersion and dissolution of the API inside a molten polymeric matrix using a Brabender batch mixer, in order to determine the dissolution kinetics of the API.

DISPERSION AND DISSOLUTION KINETICS OF API PARTICLES IN PHARMACEUTICAL HOT MELT EXTRUSION

by
Wang Zhan

A Thesis
Submitted to the Faculty of
New Jersey Institute of Technology
in Partial Fulfillment of the Requirements for the Degree of
Master of Science in Pharmaceutical Engineering

Department of Chemical, Biological and Pharmaceutical Engineering

May 2014

APPROVAL PAGE

DISPERSION AND DISSOLUTION KINETICS OF API PARTICLES IN PHARMACEUTICAL HOT MELT EXTRUSION

Wang Zhan

Dr. Costas G. Gogos, Thesis Advisor Date
Distinguished Research Professor of Chemical, Biological and Pharmaceutical Engineering, NJIT & President Emeritus of Polymer Processing Institute (PPI)

Dr. Piero M. Armenante, Committee Member Date
Distinguished Professor of Chemical, Biological and Pharmaceutical Engineering, NJIT

Dr. Robert B. Barat, Committee Member Date
Professor of Chemical, Biological and Pharmaceutical Engineering, NJIT

Dr. Nicholas Ioannidis, Committee Member Date
Research Engineer of Polymer Processing Institute

BIOGRAPHICAL SKETCH

Author: Wang Zhan

Degree: Master of Science

Date: May 2014

Undergraduate and Graduate Education:

- Master of Science in Pharmaceutical Engineering,
  New Jersey Institute of Technology, Newark, NJ, USA, 2014

- Bachelor of Science in Pharmaceutics,
  Zhengzhou University, Zhengzhou, Henan, P. R. China, 2012

Major: Pharmaceutical Engineering

I dedicate this to my beloved family.

ACKNOWLEDGMENT

I am extremely grateful to Prof. Costas G. Gogos, who not only served as my advisor, providing valuable resources, wise and strong academic guidance, but also gave me constant moral support and encouragement when I encountered problems through my MS studies. I am highly honored that I obtained advice from this esteemed and knowledgeable advisor.

I also appreciate the involvement of Dr. Nicolas Ioannidis for his instructive suggestions and discussions with me throughout my work. Special thanks are given to Prof. Piero M. Armenante and Prof. Robert B. Barat for their participation in my thesis committee.

I also want to thank the Polymer Processing Institute (PPI) for making their facilities available to me and the advice I received from the staff. I want to thank Ms. Mariann Pappagallo for her help with administrative matters as well.

Finally, I give my deepest gratitude to my parents, Xianyun Zhan and Yanran Yin. Their support, understanding, love, and sacrifice made me who I am now.

TABLE OF CONTENTS

Chapter	Page
1 INTRODUCTION……..……..……..	1
1.1 Objective …….....……..……...	1
1.2 Background Information …….…….....	2
2 LITERATURE REVIEW …….…….…….…….……	4
2.1 Pharmaceutical Hot-melt Extrusion ……	4
2.2 Distributive Mixing and Dispersive Mixing……	5
2.3 Dissolution of API Particles in Polymeric Melt ……	7
2.4 Characterization Methods……	14
2.4.1 Microscopy Methods ……	14
2.4.1 Batch Mixer ……...	15
3 MATERIALS AND METHODS……	17
3.1 Materials ……...……...……...……...……...……	17
3.2 Scanning Electron Microscopy (SEM) and Light Microscopy (LM) ……	17
3.3 Batch Mixing……..……...……...……...……...……...……	19
3.4 Angle of Repose……...……...……...……...……...……...……...	21
4 RESULTS AND DISCUSSION ……...……...……...……..……	22
4.1 Characterization of the Raw Materials ……	22
4.1.1 Angle of Repose ……	22
4.1.2 Bulk Density...……	23
4.2 Identification of a Suitable Non-Dissolving Surrogate For APAP ……	24

TABLE OF CONTENTS
(Continued)

Chapter	**Page**
4.2.1 Identification by Particle Size, Size Distribution and Particle Morphology …….……	24
4.2.2 Investigation of the Effect of Different Particle Properties on the Polymeric Melt Viscosity. …….	28
4.3 Finding the Dispersion and Dissolution Kinetics of APAP added into Soluplus Melt Matrix ……..……	31
5 SUMMARY AND FUTURE WORK ……..……	44
5.1 Summary ……..……	44
5.2 Future Work ……..……	46
REFERENCES.....	47

LIST OF TABLES

Table		Page
2.1	A Sample Data Table Gathered With a Batch Mixer.....	16
4.1	Bulk Densities of API and Surrogates…...……..……..……	24
4.2	Average Particle Size and Size Distribution of API and Surrogates …….….....	27

LIST OF FIGURES

Figure		Page
2.1	Dispersive mixing and distributive mixing of solid agglomerates and immiscible liquid droplets (Tadmor and Gogos, 2006). ……..……	7
2.2	Schematic representation of the morphological changes of the drug and polymer system in the solution formation process for Case I. ……	9
2.3	Schematic representation of the morphological changes of the drug and polymer system in the solution formation process for Case I. ..…..……...….....	11
3.1	The batch mixer (a) and roller screws (b) (Manufactured by Brabender Corp…..	19
3.2	The inside of the assembled Brabender batch mixer (without the front plate).....	20
4.1	The results of the tests of the angle of repose: (a) $CaCO_3$ No.1, (b) $CaCO_3$ No.2, (c) $CaCO_3$ No.3, (d) $CaCO_3$ No.4, (e) Soluplus, (f) Aluminum, (g) Acetaminophen (APAP)…..……	22
4.2	(a) SEM of Al, (b) SEM of Al_2O_3, (c) LM of $CaCO_3$ no.1, (d) LM of $CaCO_3$ no.2, (e) LM of $CaCO_3$ no.3, (f) SEM of APAP (g) SEM of $CaCO_3$ no.4, (h) SEM of Indometacin……	26
4.3	Torque traces of Soluplus upon the addition of different grades of $CaCO_3$ or Al....	28
4.4	Melt temperature traces of Soluplus upon the addition of different grades of $CaCO_3$ or Al.…...……...……...……...……...……...	28
4.5	Torque traces of Soluplus upon the addition of APAP and Aluminum……	31
4.6	Temperature traces of Soluplus upon the addition of APAP and Aluminum…….	31
4.7	The intermeshing roller screw elements..…..……..	33
4.8	Torque traces of Soluplus upon the addition of APAP and Aluminum (Magnified/Expanded scale)……..	34
4.9	Temperature traces of Soluplus upon the addition of APAP and Aluminum (Magnified/Expanded scale)……...	34

LIST OF FIGURES
(Continued)

Figure **Page**

4.10 The cartoon visualization for the Soluplus and APAP compounding physics..... 38

4.11 Torque traces of Soluplus upon the addition of APAP (repeat 2 times) and Aluminum (Magnified/Expanded scale)..... 40

4.12 Temperature traces of Soluplus upon the addition of APAP (repeat 2 times) and Aluminum (Magnified/Expanded scale)..... 40

4.13 The dissolution estimation by the plot of ln M vs. time..... 42

CHAPTER 1

INTRODUCTION

1.1 Objective

Pharmaceutical Hot-Melt Extrusion (HME) is currently pursued by both industry and academia as a method to produce solid oral dosages in a continuous and controlled fashion. One of the major concerns in pharmaceutical HME is the thermal degradation of the API. To achieve the balance between complete dissolution of the API and minimal thermal degradation of the API, the dissolution kinetics of the API particulates inside the molten polymeric matrix during extrusion must be known. In this work, we study the *dissolution kinetics of the API* during pharmaceutical HME by experiments, which attempt to separately determine the contributions of *polymer melting*, *dispersion/distribution of API particulates, and API dissolution* on the melt viscosity of the polymer matrix during melt-mixing in Brabender batch mixer. Since the last two of the three phenomena are taking place (at their own characteristic rate) *simultaneously*, this is not an easy task.

1.2 Background Information

Pharmaceutical hot melt extrusion (HME) is currently investigated by both industry and academia as a method for producing solid oral dosages in a continuous and controlled fashion. Processing by HME can improve the bioavailability of the poorly water-soluble active pharmaceutical ingredients (APIs) by dissolving them into water-soluble polymers (products known as *solid solutions*). At the same time, oral dosages with controlled release characteristics can be produced by dispersing water-soluble APIs into water-insoluble polymers (products known as *solid dispersions*) (G. Terife, 2012).

The elementary steps involved in the pharmaceutical HME are identical to the ones involved in conventional plastics melt processing by extrusion: (1) *handling of particulates,* (2) *melting,* (3) *dispersive and distributive mixing*, (4) *devolatilization and stripping* (5) *pressurization and pumping* (Z. Tadmor, C.G. Gogos, 2012). However, for pharmaceutical HME the *dissolution of the API* is an additional and very important elementary step, along with *melting of the polymeric excipient* that precedes it, and *mixing* which accelerates the dissolution process (C.G. Gogos, 2012).

The thermal degradation of the API is one of the major concerns in pharmaceutical HME. Producing an extrudate that contains a molecularly dispersed (i.e. dissolved) API and at the same time not overexposing the API to high processing temperature for long periods is one of the major objectives during the extrusion of solid solutions (W. Thiele, 2003) .

To achieve the balance between complete dissolution of the API and minimal thermal degradation of the API, the dissolution kinetics of the API particulates inside the molten polymeric matrix during extrusion must be known.

As mentioned above, *melting of the polymeric excipient*, *dispersive/distributive mixing*, and *API dissolution* can occur simultaneously during extrusion. Therefore to determine the dissolution kinetics of the API, the above phenomena must be isolated from each other. One way of achieving this is by exploiting the effect that *polymer melting, dispersion/distribution of API particulates and API dissolution* have on the melt viscosity of the polymer matrix: Melt viscosity *decreases* with heat. Addition of particulates in molten polymers *increases* the melt viscosity. Dissolution of an API into molten polymers generally *decreases* viscosity by virtue of plasticization.

In this work, we attempt to study the *dissolution kinetics of the API* during pharmaceutical HME by separately determining the contribution of *polymer melting, dispersion/distribution of API particulates and API dissolution* on the melt viscosity of the polymer matrix during melt-mixing in Brabender batch mixer. The strategy we followed to achieve the separate determination of the above phenomena on the melt viscosity of the polymer included: (a) pre-melting the polymer alone in the batch-mixer (b) adding and mixing a *non-dissolving*, surrogate material that has the similar particulate properties with the API, (c) melt mixing the polymer with the API, and finally, subtracting the contribution on the melt viscosity of the polymer of step (b) from step (c).

CHAPTER 2

LITERATURE REVIEW

2.1 Pharmaceutical Hot-Melt Extrusion

Hot-melt Extrusion is a term adopted by the Pharmaceutical industry to differentiate from traditional oral dosage manufacturing techniques, such as direct compression and tableting. Because of its potential of rendering poorly water-soluble active pharmaceutical ingredients (APIs) readily bioavailable to patients, both the industry and academic investigators have explored and studied it in the last several decades or so. The recent discoveries of a large number of promising, but basically crystalline, water-insoluble APIs, has resulted in more and more intensive academic and industrial investigations of HME for these Class II poorly-soluble APIs.

HME typically involves the use of single but more often than not twin rotor extruders (also referred as SSE and Co-TSE respectively) for the melting of usually water-soluble polymeric excipients, mixing them with water-insoluble APIs, and pumping the homogeneous mixture through a die to form an extrudate. HME is a solvent-free continuous process and may lead to fewer processing steps, compared to the traditional drug production processes. Degradation of the drug (API) and excipient may occur during HME because of the high processing temperatures and heating which is due to

viscous energy dissipation (VED). Hence it is a serious concern and an area which is addressed in studies exploring the suitability of HME for new API/excipient systems.

Pharmaceutical HME can be generally divided into two categories with the respect to the processing temperature. In the most common case (Case I), the processing temperature ought to be over the melting temperature of semi-crystalline polymers or (50-100)℃ above the glass transition temperature of amorphous polymers but below the melting temperature of the crystalline API. While in the other case (Case II), the processing temperature is above the melting temperature, the glass transition temperature of the polymer and the melting point of the API (C.G. Gogos, 2012). Typically, Case I is more preferred, since it means minimizing the chances of thermal degradation of the API.

In general, HME involves five elementary steps: handling of particulate solids, melting, pressurization and pumping, mixing, and devolatilization and stripping (Tadmor and Gogos, 2006). Mixing plays a critical role in determining the key properties of final products, mainly in part of the API dissolution rate in the aqueous polymer or other medium.

2.2 Distributive Mixing and Dispersive Mixing

Mixing in single or twin screw extruders is induced by laminar flow and is generally categorized into two types: dispersive mixing and distributive mixing. Dispersive mixing

refers to the process involving the particle size reduction of particulate cohesive components such as fillers, polymer gels, or liquid droplets. Distributive mixing refers to expanding and stretching the interfacial area between the components lacking a cohesive force in between and distributing them uniformly throughout the volume of the molten polymer. Dispersive mixing is mainly controlled by the laminar shear and extensional forces and the type of flow generated by the processing equipment. On the other hand, distributive mixing is mainly controlled only by the flow-generated strains. According to the definitions, the mixing of miscible liquids is treated as distributive mixing, and mixing of hard solid agglomerates, immiscible liquids, and soft agglomerates is regarded as dispersive mixing (Tadmor and Gogos, 2006). The dispersive and distributive mixing of solid agglomerates is schematically shown in Figure 2.1. As the figure shows, the upper route is when the dispersive mixing happens before the distributive mixing and the lower route is the other way around.

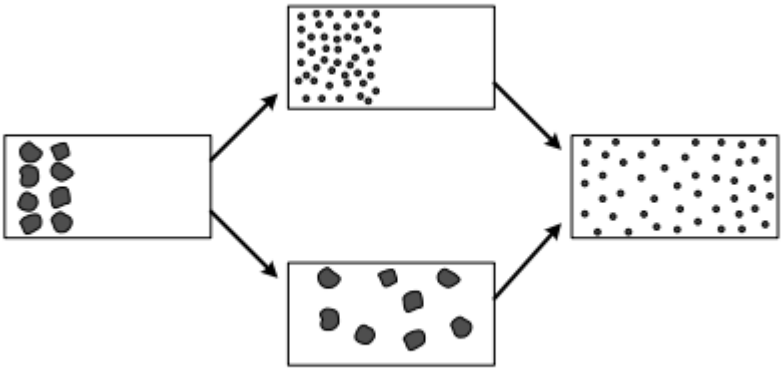

Figure 2.1 Dispersive mixing and distributive mixing of solid agglomerates and immiscible liquid droplets (Tadmor and Gogos, 2006).

Source: Z. Tadmor, C. G. Gogos (2006). *Principles of Polymer Processing*, John Wiley & Sons, Inc. Hoboken, NJ, USA.

2.3 Dissolution of API Particles in Polymeric Melt

The dissolution of API within the polymer largely depends on their physicochemical properties. Good miscibility between APIs and polymer excipients is the key requirement for solid dispersions to increase physical stability (Patrick J. Marsac, 2008). In practice, the majority of drug/polymer systems are likely to show only partial miscibility (Craig, 2002). This means that there exists a certain thermodynamic solubility of drugs in polymer matrixes.

HME can be carried out in two distinctly different conditions, referred to here as Cases I and II:

Case I: The processing temperature is above the melting temperature for a semi-crystalline polymer, or the softening temperature for an amorphous polymer, (Tg + 50~100 ℃) but below the melting point of a drug.

Case II: The processing temperature is above both the melting temperature and the softening temperature of semi-crystalline or amorphous polymers, respectively, and above the melting point of a drug. One thing needed to be noted that processing temperature should be the melt temperature instead of the set temperature of the processing equipment. It should also be noted that the incorporation of the API may decrease the glass transition temperature of an amorphous polymer or the melting temperature of a semi-crystalline polymer (Crowley et al., 2007).

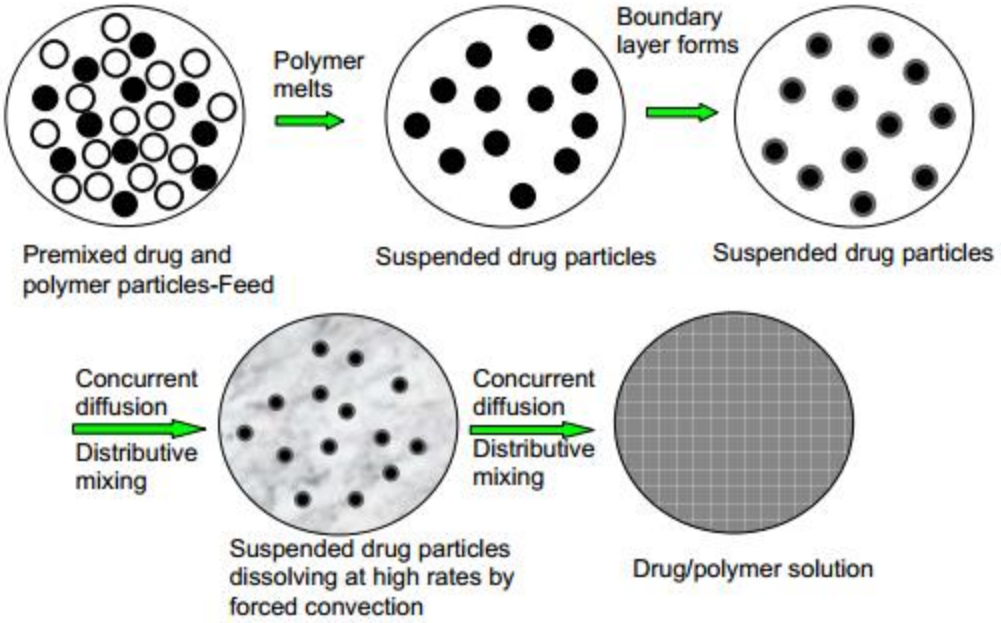

Figure 2.2 Schematic representation of the morphological changes of the drug and polymer system in the solution formation process for Case I.

Case I provides a viable method to circumvent the thermal degradation issues. In case I, the drug is processed below its melting point and mixed with a polymer melt, then the solid drug particles gradually dissolve into the polymer excipient melt. And this process should be able to provide a desirable polymer-drug solid dispersion or solid solution. In other words, the solid API is the solute and the polymeric melt is a highly viscous solvent, during the HME process. In addition, with higher temperature, the dissolution rate and solubility of the API in the polymer will increase.

The dissolution process of the drug in the polymer melt is schematically shown in Figure 2.2. Firstly, the drug particles (black) and polymer particles (white) are fed into the batch mixer or an extruder. Then, the polymer particles start melting due to the conductive heat

from the mixer or extruder barrel and frictional and plastic energy dissipation. These two phenomena result in a process charge state that the solid drug particles are suspended in a continuous polymer melt matrix. Then the polymer molecules start to heat up the API particles and create a mass transfer boundary layer. This layer shall be continuously wiped away and replaced with fresh polymer melt nearby. The drug molecules diffuse into the polymer melt through the boundary layer, and the size of the suspended drug particles will continue to decrease as the diffusion goes. Finally, a homogeneous *solution* will be formed.

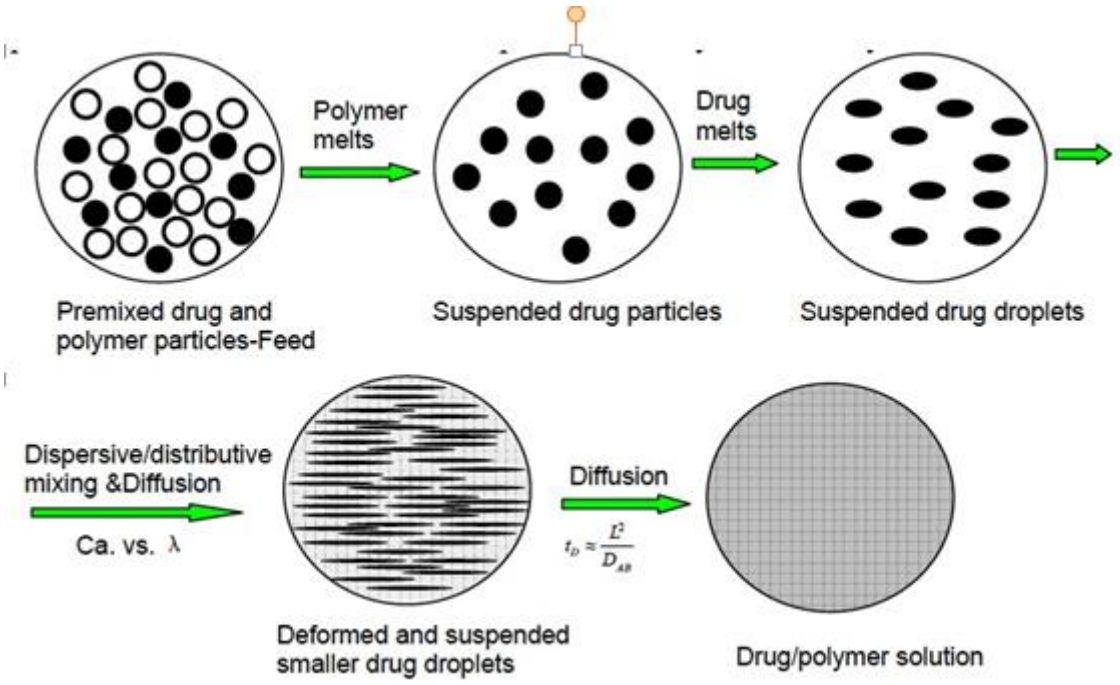

Figure 2.3 Schematic representation of the morphological changes of the drug and polymer system in the solution formation process for Case II.

Case II, on the other hand, includes miscible or partially miscible liquid-liquid mixing because both the polymer and drug will be melted. As shown in Figure 2.3, the drug (black) and polymer (white) particles are fed into an extruder and processed by the screw elements. Due to the heat transfer from the extruder barrel or a batch mixer, and frictional and plastic dissipation, the polymer particles will melt first. During or after the melting of the polymer, the drug particles will melt to droplets and be deformed by the mixing flows generated by the screws. The droplets will be deformed along the shear direction and blurred the contacting surface between the drug and polymer. As this process goes on and with diffusion continuously being carried on, we will finally get a homogeneous drug – polymer solution.

In both cases discussed above, the diffusion will happen, between either the dissolving API particles or the drug droplets and the molten polymer.

The "characteristic diffusion time" t_D is proportional to the square of the API phase droplet or ligament radius L or the thin dimension D_{AB} of a sheet (Equation 2.1).

$$t_D = \frac{L^2}{D_{AB}} \tag{2.1}$$

In HME, similarly, the dissolution of drug particles in molten polymer excipients can be described by the Noyes- Whitney equation as follows:

$$\frac{dC}{dt} = \frac{D \times A \times (C_s - C)}{h \times V} \tag{2.2}$$

where D is the diffusion coefficient of drug; A is the total surface area of the drug exposed to the dissolution media; C_s is the saturation solubility of the drug in the liquid which (for HME) is the excipient melt; C describes the concentration of the dissolved solid phase in the bulk at time t; h represents the diffusion boundary layer at the solid – liquid interface; and V is the volume of the dissolution medium.

The equation shows that the drug particle size and size distribution are very important to the dissolution rate, since the total contacting surface area of the drug particles will be changed accordingly. We can expect a higher dissolution rate if the particle size gets smaller. Furthermore, the narrower the drug particle size distribution, the more uniform

the total dissolution time distribution needed for complete dissolution of drugs in polymer melt will be. (Gogos, 2012)

Dispersive mixing may break up the drug agglomerates or even individual particles due to the high shear forces generated by the high shear screw elements such as wide kneading blocks or Maddock elements (Tadmor and Gogos, 2006). Then, the total contacting surface area of the drug particles to the polymeric melt will be increased, thus increasing the dissolution rate. Distributive mixing can homogenize the drug concentration dissolved in the polymeric melt, and bring more polymer melt into contact with the suspended drug particles. Both effects can raise or maintain the dissolution rate.

If the mixer set temperature increases, on the one hand, the diffusion coefficient will increase due to the increased temperature and resultant decreased matrix viscosity; on the other hand, C_s also will increase. Both of these factors will contribute to an increase of the API dissolution rate in the molten polymer excipient. When the screw speed increases, the distributive mixing is improved within the chamber, and thus a higher concentration gradient around the drug particulates is available. Moreover, the thickness of the mass transfer boundary layer decreases as the screw speed increases. Both effects lead to an increased dissolution rate.

2.4 Characterization Methods

2.4.1 Microscopy Methods

Optical and electron microscopy can help determine the existence of drug crystal regions and the size. Although the resolution of polarized light microscopy (PLM) is approximately at 1μm, the birefringence of the crystal drug imparts a sharp and distinct contrast against the amorphous (dark) excipient. Yoo et al. studied the miscibility/stability for 24 binary solid dispersion systems and found that the sensitivity to crystal detection was PLM > DSC (Differential scanning calorimetry) > XRD (X-Ray Diffraction) (Yoo S.U., 2009). Bruce et al. employed SEM for in-situ observation of crystal growth in melt extrudates (Bruce C., 2007).

SEM makes use of a beam-scanning mode of operation. A fine electron beam scans the surface of the specimen previously coated with a conducting layer in a two-dimensional raster. The back-scattered or the secondary electrons are analyzed with a scintillation counter, and the signal from the counter is fed into a cathode-ray tube which is set to scan synchronously with the electron beam. As a result, a point-by-point image of the specimen is displayed on the cathode-ray tube. In order to increase the electric conductivity of the tantalum layer, a subsequent carbon layer has to be deposited by flash evaporation of carbon yarn (W. Doll, 1985).

2.4.2 Batch Mixer

The batch mixer is a heated high-shear laminar mixer, and it has been used in the plastics and rubber industry to simulate the extrusion process or optimize the formulation. This laboratory scale batch mixer used in this work needs only 30-60 g of the material. With the equipment, many experiments can be performed in a short period, thus making it an attractive choice for the HME study (Ghebre-Sellassie and Martin, 2007). Furthermore, the screw speeds can be controlled separately without altering the residence time in a batch mixer, which is difficult to realize if an extruder is used.

The Bradender batch mixer used in this work can be applied for the determination of thermoplastics, thermosets, elastomers, ceramic molding compounds, fillers, pigments and much more plastic and plastifying materials under praxis-oriented conditions, cost-effective, reliable and little expenditure of time and material.

As for the measurement, the principle is based on making visible the resistance the sample material opposes to the rotating blades. The corresponding torque moves a dynamometer out of its zero position.

In compliance with the existing standards and test specifications, a typical 'Plastogram®' (torque and stock temperature vs time) is recorded for each sample material. This diagram shows the relationship between torque (viscosity) and temperature/time in consideration of structural changes of the material. The measured data are displayed

Table 2.1 A Sample Data Table Gathered With a Batch Mixer.

Time [s]	Torque [Nm]	Temperature [℃]	Speed [rpm]
0	0	130.5	50.3
2	1.201789	87.7	50.4
4	2.724987	87.9	50.5
6	3.926776	88.6	50.5
8	13.6948	91.2	50.5
10	30.12857	96.7	50.5
12	54.89101	113.5	50.4
14	56.60985	120.3	50.4
16	56.60985	129.7	49.7
18	53.18615	132.2	50.5
20	51.11795	134.4	50.6

numerically as a table and/or graphically as a diagram during the measurement on a monitor and can be printed and stored. A sample of typical data table is shown in Table 2.1.

CHAPTER 3

MATERIALS AND METHODS

3.1 Materials

Acetaminophen (APAP) (Spectrum Chemicals, Gardena CA) was chosen as the model API. APAP is a crystalline BCS I drug with a melting point of 169 ℃. Soluplus (BASF, Tarrytown NY) was used as the model polymeric excipient. It is an amphiphilic polyvinyl caprolactam-polyvinyl acetate-polyethylene glycol graft copolymer and is amorphous with a single glass transition temperature (Tg) of 73 ℃ ± 2 ℃ that exhibits pH-independent solubility in water. According to the criterion described in the literature (Greenhalgh D.J, 1999) (Forster A., 2001), APAP and Soluplus are likely to be miscible.

Al, Al_2O_3 and four grades of $CaCO_3$ were evaluated in terms of particle size/size distribution as non-dissolving surrogates for APAP. The 4 grades of $CaCO_3$ will be referred as $CaCO_3$ No.1 to 4 respectively according to the descending order of the average particle size printed on the brand tags.

3.2 Scanning Electron Microscopy (SEM) and Light Microscopy (LM)

Scanning Electron Microscopy (SEM) and Light Microscopy (LM) were used to determine the particle/particle size distribution of the all particulates used in this work.

To obtain representative results, 200 particle measurements were obtained from each material (diameter-based measurements using image-processing ImagePro 6.0).

To determine the particle size distribution of the finer $CaCO_3$, Aluminum, Al_2O_3, APAP, DMN and Indometacin, we use a scanning electron microscope (LEO Field Emission Gun 153 Digital SEM) operated at an accelerating voltage of 10 KeV. All samples except Aluminum were coated with a thin layer of carbon using a Bal-Tee Med 020 Sputter Coater in order to improve the electrical conductivity before imaging.

Likewise, to determine the particle sizes and distributions of the coarser $CaCO_3$ grades, we use a light microscope (Dino-Lite Pro digital microscope along with the Dino Capture 2.0 software) since the particles are large enough to observe with a light microscope.

3.3 Batch Mixing

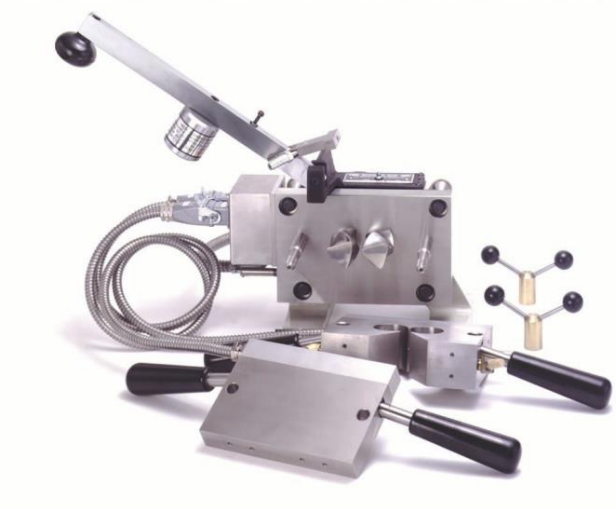

(a)

(b)

Figure 3.1 The batch mixer (a) and roller screws (b) (Manufactured by Brabender Corp.)

Source: Liu, H. (May 2010). Hot Melt Mixing/Extrusion and Dissolution of Drug (Indomethacin) in Acrylic Copolymer Matrices. Otto H. York Department of Chemical, Biological and Pharmaceutical Engineering. Newark, New Jersey Institute of Technology. Ph.D Dissertation.

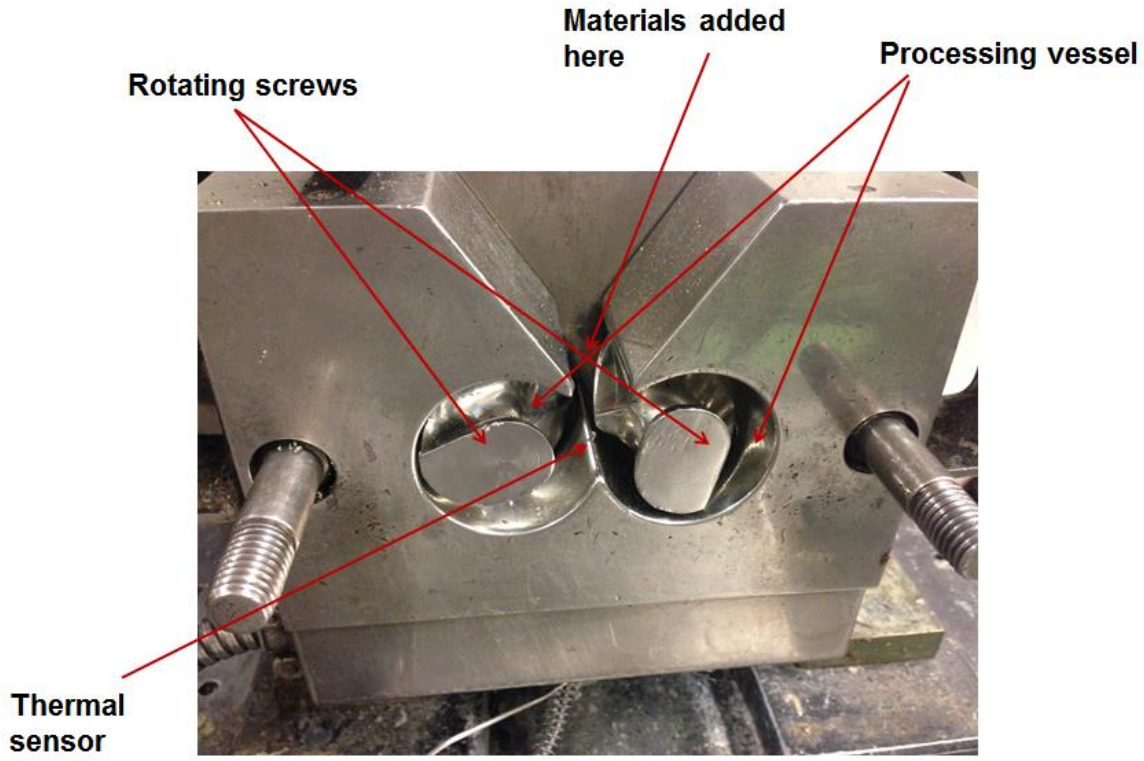

Figure 3.2 The inside of the assembled Brabender batch mixer (without the front plate).

A Brabender batch mixer (Shown as Figure 3.1 and 3.2) was used for compounding of the materials.

All the experiment runs were performed in a Brabender FE-2000 batch intensive mixer utilizing counter-rotating screws, as illustrated in Figure 3.1. During mixing the torque arising from the resistance of material to the flow created by the counter-rotation of the screws, is recorded along with the melt temperature. The batch mixer barrel is heated with electrical power and cooled down by air.

All the materials were mixed at 50 rpm for 20 min, while the set temperature of the mixer was 130 ℃. The polymer will be processed for 10 minutes before we add the additive. The weight ratio of the materials was kept constant in all experiments at 70/30 polymer/additive (exceptions will be noted when discussed about).

3.4 Angle of Repose

The angle of repose for a granular material is the steepest angle of descent or dip relative to the horizontal plane, where the material can be piled without slumping. The angle of repose is measured by a Hosokawa powder tester (PT-N) to characterize the flowability of all the particles used in the experiments carried on in the batch mixer, i.e. Soluplus, APAP, Aluminum and all 4 grades of $CaCO_3$. The procedure used was the following steps:

Obtain approximately a 250g sample of the powder which should be homogeneous and representative of the bulk material. Place the material in the jar container on a funnel over the base plate. Feed the powder into the funnel until nearly full. Start adding the powder into the funnel at a rate similar to its discharge rate. When the edge of the sample powder pile reaches the edge of the plate, stop feeding the powder. Using the calipers, measure the height of the cone. Return the tested specimen to the jar container and remix to homogenize. Repeat these steps two more times for each kind of powder and calculate the average of the angle of repose.

CHAPTER 4

RESULTS AND DISCUSSION

4.1 Characterization of the Raw Materials

4.1.1 Angle of Repose

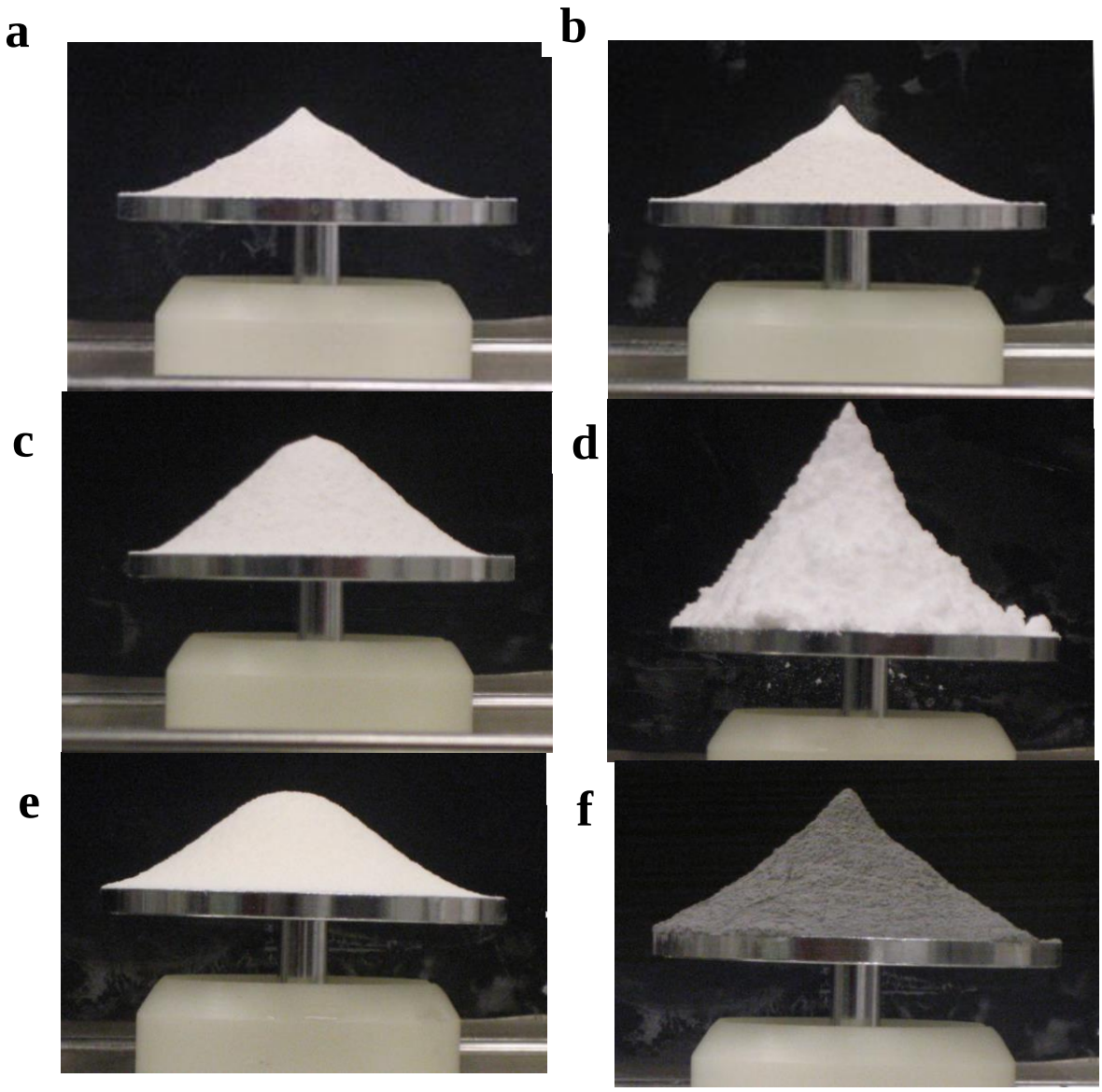

g

Figure 4.1 The results of the tests of the angle of repose: (a) $CaCO_3$ No.1, (b) $CaCO_3$ No.2 , (c) $CaCO_3$ No.3, (d) $CaCO_3$ No.4, (e) Soluplus (f) Aluminum (g) Acetaminophen (APAP)

All the raw materials used in the Brabender batch mixer experiments are shown as above (Figure 4.1) (the respective particle sizes of the materials can be found in Table 4.2). From the pictures we can see that the $CaCO_3$ No.1 has the angle of repose which is around 25°, while the $CaCO_3$ No.2 and $CaCO_3$ No.3 are about 30°, and $CaCO_3$ No.4 is 40°. And The angle of repose for Soluplus is about 25°, for Aluminum is around 30°. APAP has the largest angle of repose which is about 70°, indicating it has the worst flowability among all the materials.

4.1.2 Bulk Density

The bulk density of all the materials used in the Brabender batch mixer experiments are shown in the table below.

Table 4.1 Bulk Densities of API and Surrogates

Material	**Bulk Density**
[-]	[g/cm^3]
Aluminum	1.23
$CaCO_3$ No.1	1.44
$CaCO_3$ No.2	1.45
$CaCO_3$ No.3	1.44
$CaCO_3$ No.4	0.46
APAP	0.37

4.2 Identification of a Suitable Non-Dissolving Surrogate for APAP

4.2.1 Identification by Particle Size, Size Distribution and Particle Morphology

During the addition of a soluble, particulate component in a molten polymeric matrix, distribution/dispersion of the particulates and concurrent/subsequent dissolution of the particulates take place. To determine the contribution of distribution/dispersion of the API on the melt viscosity alone, the particle size/size distribution of a number of insoluble, inorganic surrogates were determined by SEM or LM. Figure 4.2 shows the SEM/LM images of all the particles examined in this work. Table 4.2 summarizes the

average particle size and standard deviation of all the particulate materials as measured by the SEM/LM images.

The increase in the melt viscosity of a polymer upon the addition of particulates depends not only on the particle size/size distribution but also: the volume fraction, the surface tension, the specific heat capacity and the aspect ratio of the added particles (Z. Tadmor, C.G. Gogos, 2012).

From the results in Table 4.2 it can be seen that in terms of size and size distribution the Al particles are closer to the APAP particles (av. particle size: 10 μm, s. deviation: 7 μm for APAP and av. particle size: 8.5 μm, s. deviation: 3.5 μm for APAP). The literature mentions that the effect of aspect ratio of added particles to the melt viscosity of a polymer becomes noticeable when the aspect ratio exceeds critical value of 10 (Z. Tadmor, C.G. Gogos 2012). From Fig. 4.2a and Fig.4.2f it can be seen that the Al particles are spherical whereas the APAP particles are cuboid in shape with an aspect ratio of ~1:6. Therefore in terms of aspect ratio the Al particles are a suitable surrogate for APAP. However, Al and APAP have different densities, specific heat capacities and surface tensions. It is therefore very difficult to find an exact surrogate for APAP and consequently, assumptions and compromises have to be made.

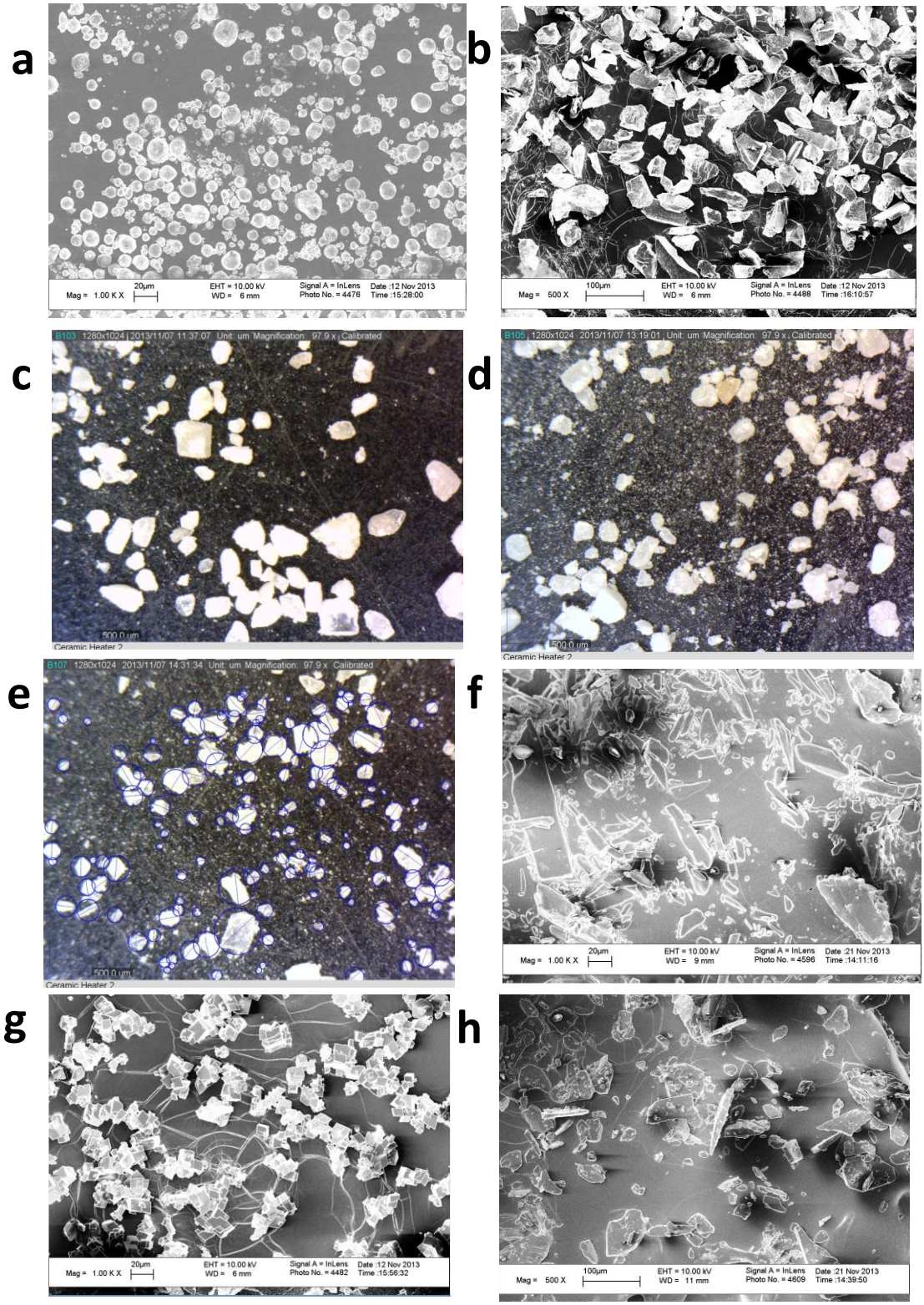

Figure 4.2: (a) SEM of Al, (b) SEM of Al_2O_3, (c) LM of $CaCO_3$ no.1, (d) LM of $CaCO_3$ no.2, (e) LM of $CaCO_3$ no.3, (f) SEM of APAP (g) SEM of $CaCO_3$ no.4, (h) SEM of Indometacin

Table 4.2 Average Particle Size and Size Distribution of API and Surrogates

Material	**Average Particle Size**	**Standard Deviation**
[-]	[µm]	[µm]
APAP	10	7
Al	8.5	3.5
Al_2O_3	37	9.5
$CaCO_3$ [no.1]	306	162
$CaCo_3$ [no.2]	260	101
$CaCO_3$ [no.3]	200	98
$CaCO_3$ [no.4]	30	20
Indomethacin	20	14

4.2.2 Investigation of the Effect of Different Particle Properties on the Polymeric Melt Viscosity

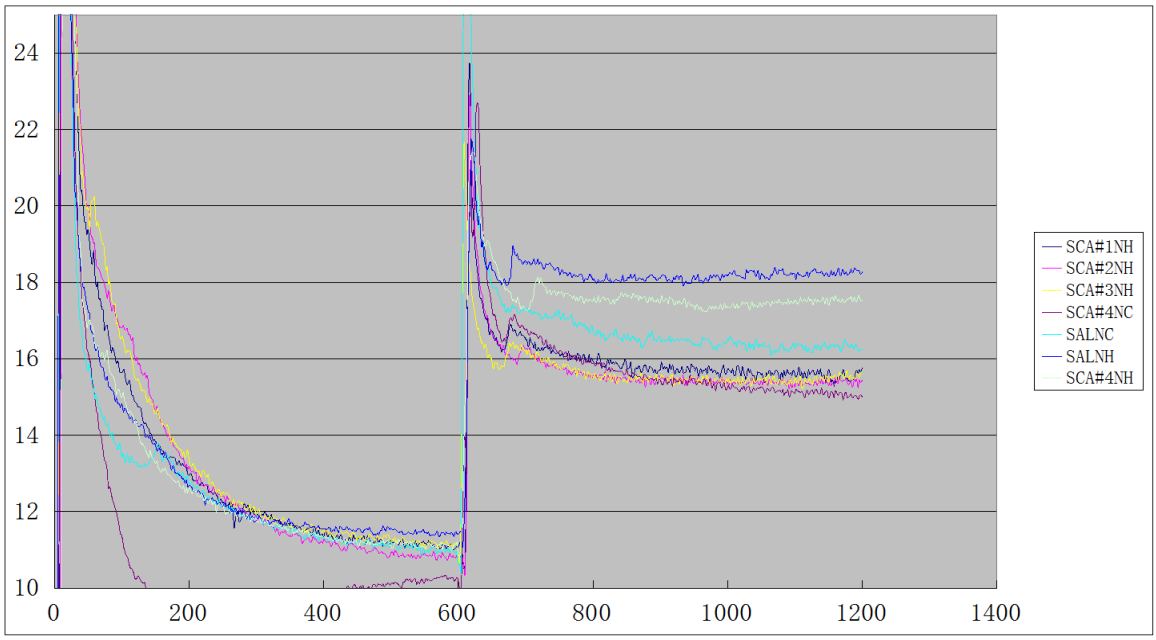

Figure 4.3 Torque traces of Soluplus upon the addition of different grades of $CaCO_3$ or Al.

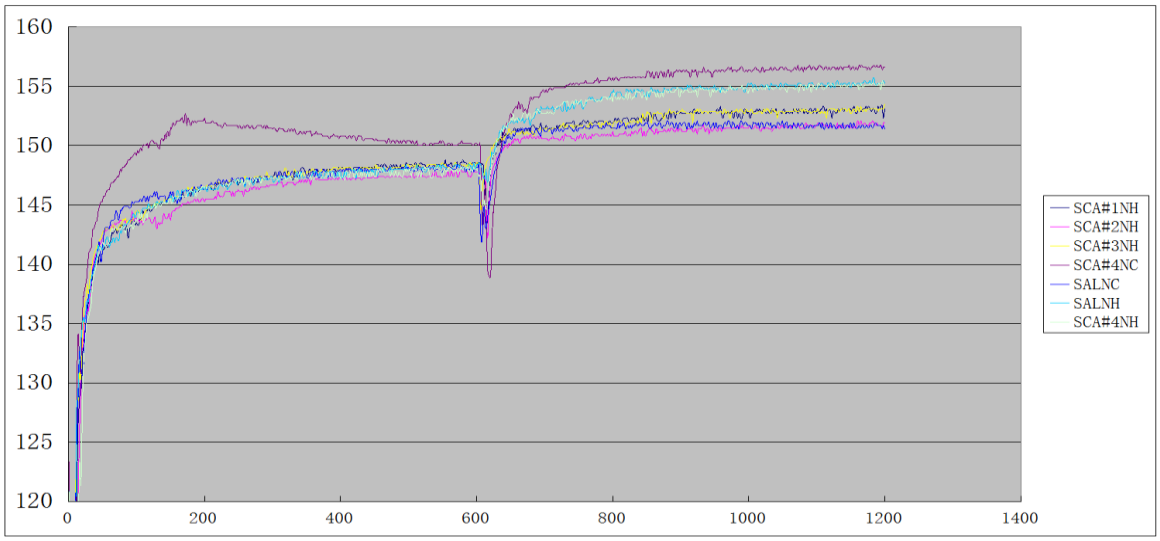

Figure 4.4 Melt temperature traces of Soluplus upon the addition of different grades of $CaCO_3$ or Al.

To determine the validity of the assumptions made and effect of compromises for particle properties on their effect on melt viscosity and identify a suitable surrogate for APAP, we decided to investigate the effect of different particle properties on the melt viscosity of Soluplus during melt mixing.

Fig. 4.3 and Fig. 4.4 show the torque and temperature traces of pre-molten Soluplus upon the addition of different grades of $CaCO_3$ or Al. In this set of experiments, we investigated two properties: particle size/size distribution and pre-mix temperature of the additive particles. In Fig. 4.3 it can be seen that the torque traces recorded during the addition of *pre-heated* (to processing temperature inside a laboratory oven) $CaCO_3$ in sizes of 200, 260 and 300 μm (termed as SCA #1NH, #2NH, #3NH respectively) are *practically identical*, indicating that the size difference between them is not sufficient to process a notable effect in melt viscosity. However when particles like $CaCO_3$ #4 (referred to as SCA #4NH as preheated compared to SCA #4NC at RT) or Aluminum (referred to as SALNH as preheated compared to SALNC at RT) $CaCO_3$ with 30 μm particle size was added the resulting viscosity increased. This is almost certainly a result of the *much larger surface area that the small particles have,* that in turn results into higher contact area between the particles and the polymer. A difference in the resulting viscosity of the polymer melt was observed when we preheated the particles to the processing temperature before adding them in the mixer. It appears that preheating the particles results into a higher viscosity melt as opposed to adding the particles at room

temperature. This may be related to the fact that heated particles are easier to become "wetted" by the polymer since the local viscosity and surface tension of the polymer around a heated particle will be lower compared to a colder particle. The reason for that is, if the particles, which are in agglomerated form when fed, are cold, then the polymer melt next to them will be cold and will not flow, mainly allowing flow of the pure melt. The extensive wetting the hot particulates, on the other hand, results in a greater and efficient contact between the particles and the melt, leading to de-agglomeration, and an increase in the melt viscosity of the Polymer/Particulate suspension.

4.3 Investigating the Dispersion and Dissolution Kinetics of APAP Added into Soluplus Melt Matrix

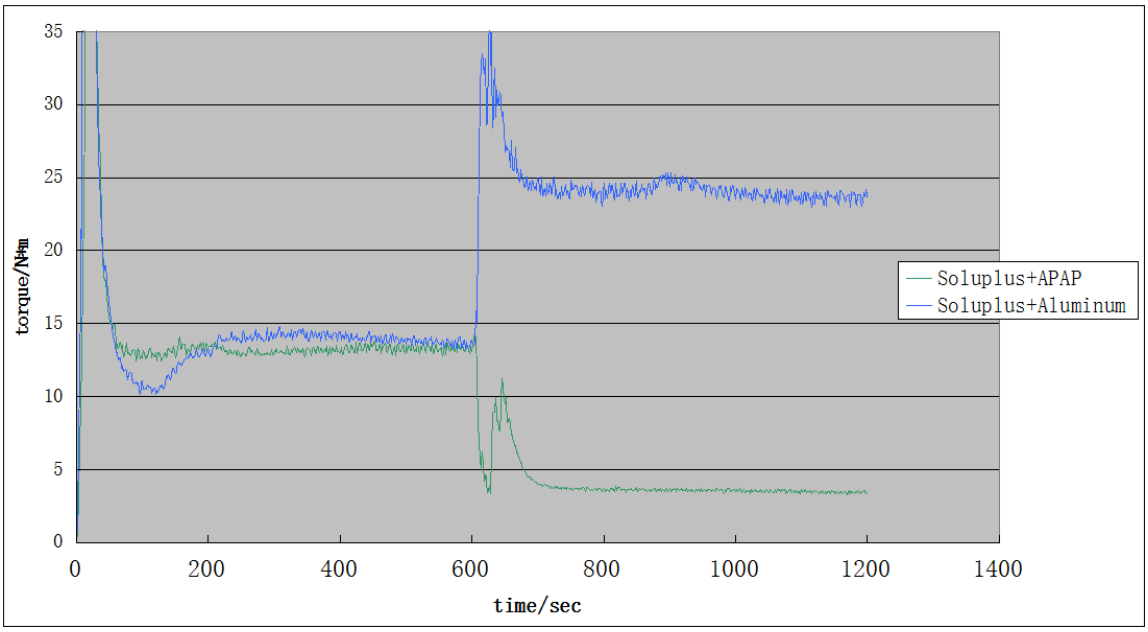

Figure 4.5 Torque traces of Soluplus upon the addition of APAP and Aluminum.

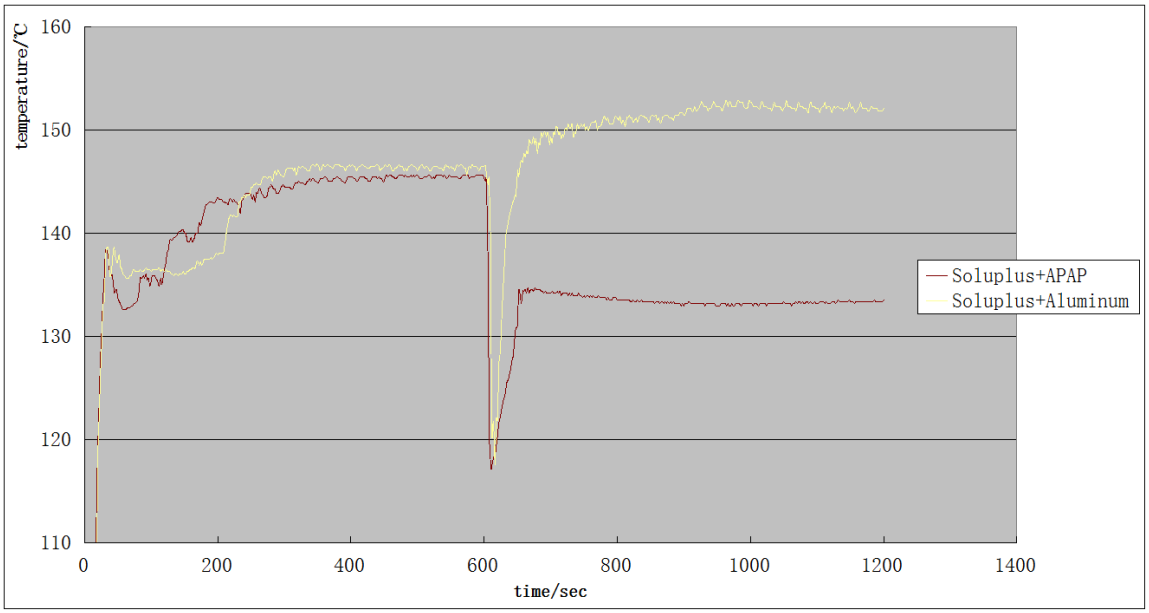

Figure 4.6 Temperature traces of Soluplus upon the addition of APAP and Aluminum.

After the screening and comparison of the results above, we decided to select and use Aluminum as the surrogate particulates and proceed to the next stage of the experiments. In this stage we took the same Brabender batch mixer runs in basically the same procedure with the previous experiments. This means the materials would still be mixed at 50 rpm for 20 min, while the set temperature of the mixer would be maintained at 130℃ and the additive will be added at 10 min. The only changed conditions are as followed.

First, we *changed the fixed weight ratio* which was Soluplus/surrogate 70/30, *into the fixed real volume ratio*, as Soluplus/Aluminum or APAP 100/36.9. And the mass of Soluplus is also fixed simultaneously because of the total volume of the batch mixer (meaning the total volume of the material) will not be altered. The reason to take such a change is in order to ensure the same real volume of the API/surrogate and Soluplus between the different runs. Since the particle sizes of Aluminum and APAP are very similar, the numbers of particles dispersed within the polymer are expected to be approximately same.

Second, the roller screws were changed into the intermeshing screw elements, as Figure 4.7 shows. The reason will be demonstrated and discussed in the next section. Since in this stage of the experiment, the condition of the usage of the screw elements is consistent for both runs, the model of screws itself shouldn't alter the results and conclusion.

Figure 4.7 The intermeshing screw elements.

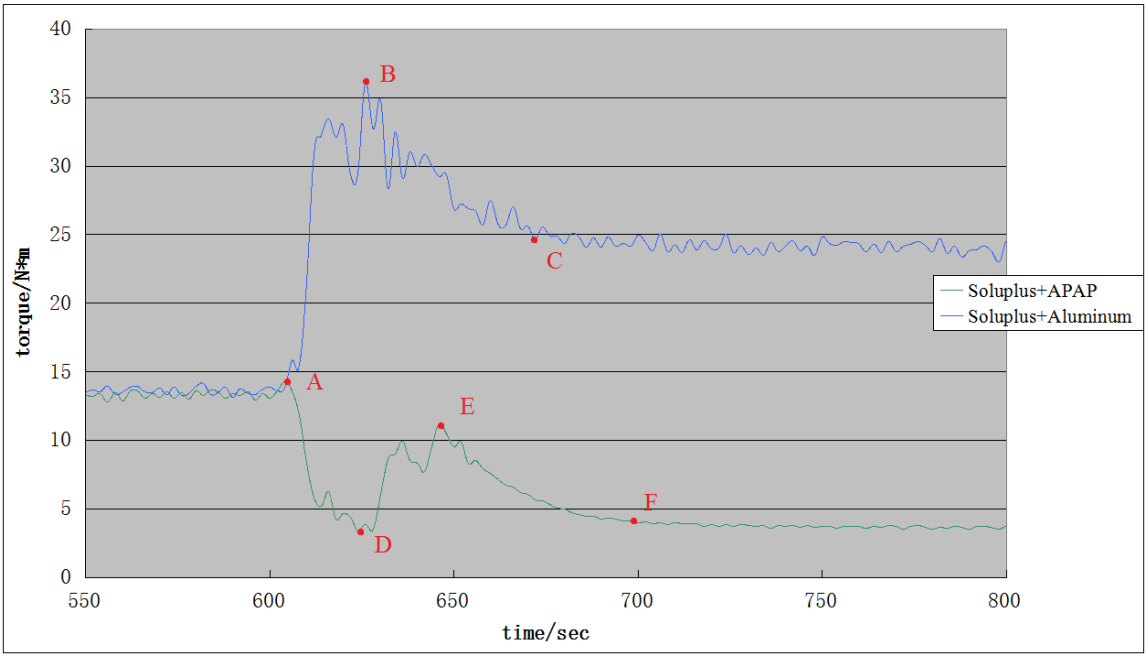

Figure 4.8 Torque traces of Soluplus upon the addition of APAP and Aluminum (Magnified/Expanded scale)

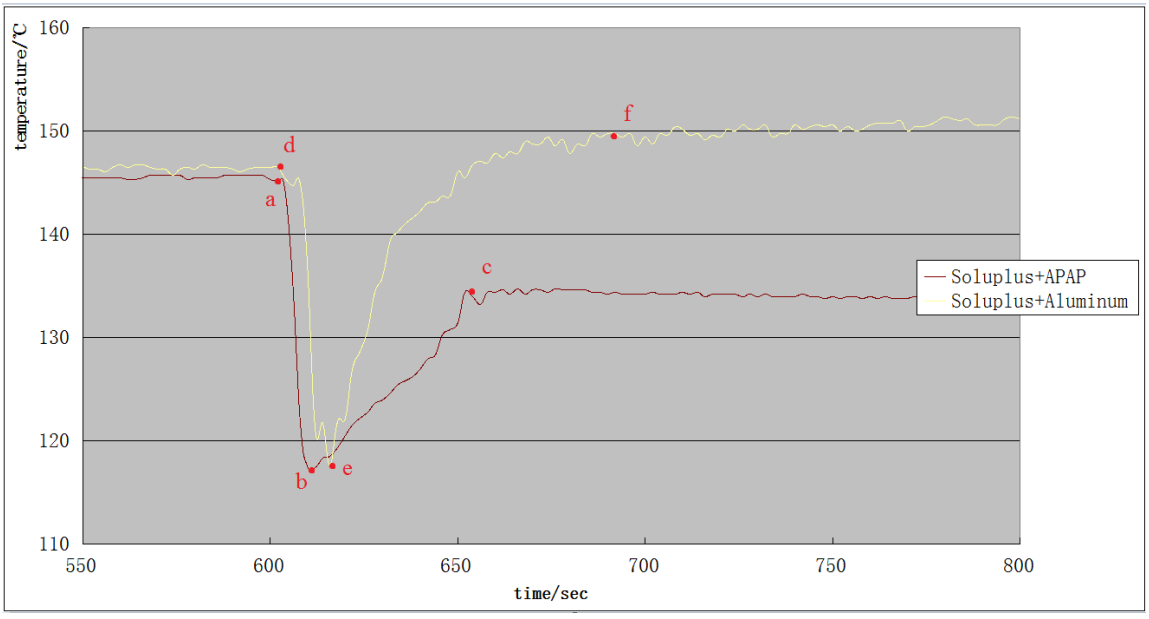

Figure 4.9 Temperature traces of Soluplus upon the addition of APAP and Aluminum (Magnified/Expanded scale)

The torque and temperature traces of these batch mixer runs are demonstrated in Figure 4.5 and 4.6 respectively and the magnification of the key parts (Specified areas of the curves in the time range between 550s and 800s) are shown in Figures 4.8 and 4.9. The torque fluctuation before the point of the maximum torque after the surrogate/API added represents the feeding surge or the occurrence of melting on the particle surface. The equilibrium torque is associated with the apparent viscosity of the drug/polymer melt mixture in the mixing chamber. The difference between the set temperature and the actual melt temperature is related to flow-induced viscous energy dissipation (VED), which depends on the mixture viscosity and the screw speed. The relation between VED and the viscosity is as in the equation below (Z. Tadmor, C.G. Gogos, 2006) :

$$VED = \eta\gamma^2 \tag{4.1}$$

Where η represent viscosity and γ is the shear flow rate. Since the screw rotational speed is set in the machine and being constant, the flow rate is also treated as constant. Then the VED should be proportional to the viscosity of the melt mixture.

We can use this equation to test the points on the curves. For example, at the start point of the surrogate/API addition, the temperatures for both polymeric matrices (point *a* and *d* in Figure 4.9) are almost the same which are around 145℃ (15℃ above the set temperature for the batch mixer) while the torques of them (point *A* in Figure 4.8) are about 14N*m. And when they reach the equilibrium, the torque is about 24N*m (point *C*

and hereafter in Figure 4.8) for the Al-Soluplus mixture and around 3.7 N*m (point F and hereafter in Figure 4.8) for APAP-Soluplus mixture. The temperatures at the equilibrium are 22 ℃ and 3.2 ℃ above the set temperature 130 ℃ for Al-Soluplus and APAP-Soluplus polymeric matrices respectively. So for each time point we mentioned above, we have the ratios of the raise of the temperature (related to VED) and torque of the matrix (related to viscosity) are 15:14, 24:22, 3.7:3.2 respectively, according to the order of the time points we have narrated above. These ratios are generally very close to each other and hence have followed the relation of the VED and viscosity demonstrated in the equation. So here through this method we can address the point that the data and the curves obtained from the experiments are quite solid and can be applied.

From the Figure 4.8, because the all the conditions are same before 600 seconds where we added the APAP/Al and the torques at point *A* are almost identical as well, we can treat point *A* as the point of starting addition of the APAP/Al for both experiments. For the part of the curve which is from point *A* to point *C* (referred as *AC*, the others applied accordingly), it takes about 75 seconds to reach the equilibrium, while for APAP curve, the *AF* part, it takes about 100 seconds. Because there's no dissolved phase in the processing of Aluminum particles, this extra period of time indicates the dissolution finished later than the dispersion phase. Compared to the temperature trace curve, we can see that from point *c* in Figure 4.9 (at about 650 seconds from the beginning), the APAP-Soluplus mixture reached at a stable temperature which is about 133 ℃.

Simultaneously, the trace of the torque also reached a peak at about 650 seconds and start to decrease hereafter. In comparison, the curves of Aluminum didn't act identically. So it's presumed that from about 650s to 700s (*EF* on the torque curve), the dispersion of the APAP within Soluplus has already been finished and there was generally only dissolution carried on during this time period. The reasons are, as we know, that the viscosity of the polymer matrix will increase through dispersion and distribution of the suspended particulates, and decrease as dissolution proceeds.

Hence, it's also obvious that after the point *F* (about 700s), both the torque and temperature reaches equilibrium, indicating both dispersion and dissolution has finished and there's only homogeneous Soluplus with dissolved APAP in the mixing chamber.

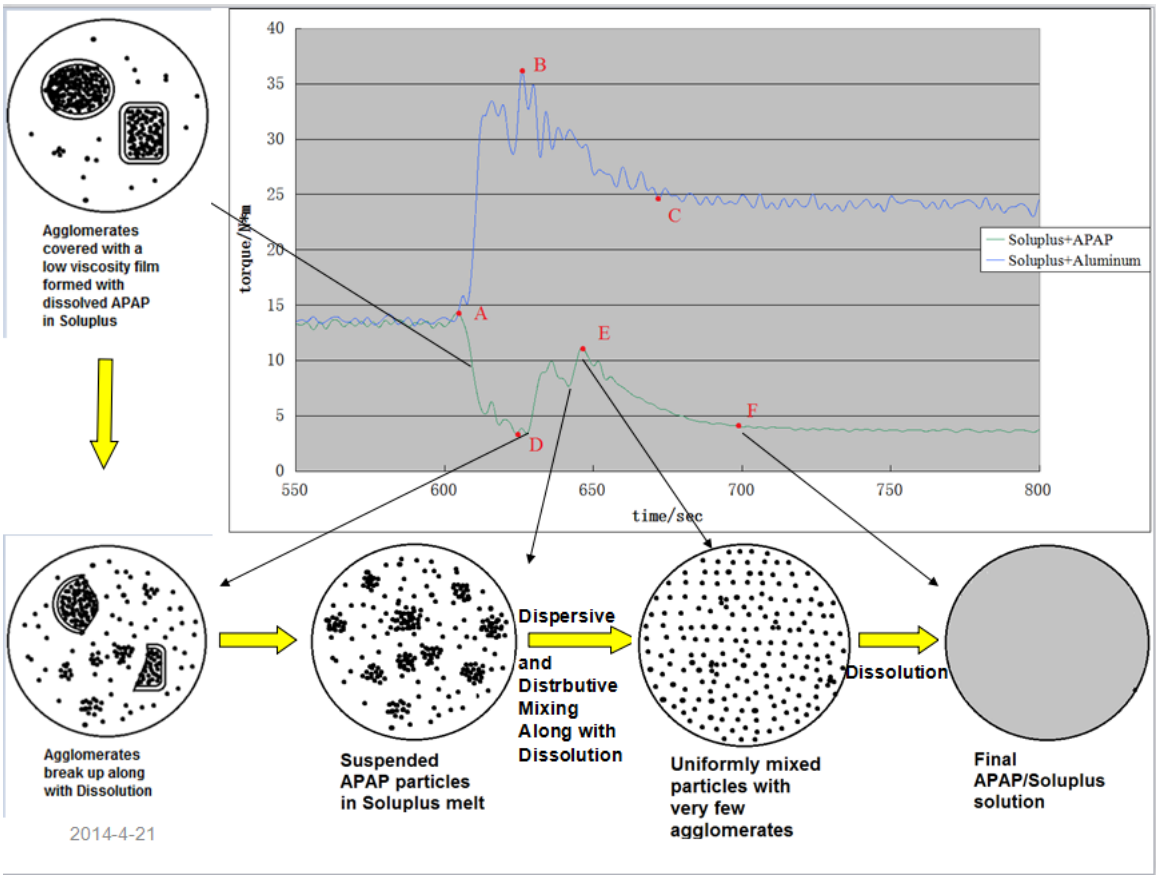

Figure 4.10 The cartoon visualization for the Soluplus and APAP compounding physics.

As for the initial torque drop at the point when the APAP was added (600s), it is presumed that the API particles were agglomerated, and because of the high temperature difference (130℃ compared with room temperature around 20℃) at the contacting surface, the APAP began to dissolve into the polymer and started to form a film covering the agglomerates. This film has a *relatively low viscosity* compared to either the polymer melt itself or the Soluplus-solid APAP matrix formed afterwards. So it starts to work as a *local plasticized/slip layer* and result in a significant drop of the viscosity. This "slip layer" effect is appreciable, and if the shear forces generated from the rotating screws is not enough to break the agglomerates and the formed film itself, the viscosity of the

mixture would even drop further. As a matter of fact this was the exact reason why we changed the configuration/design of the counter-rotating screw elements (as mentioned above) in this section of the experiment, because the non-intermeshing screws (Figure 3.1 b) that we used in the previous stage of the research couldn't generate the shear forces to break up the agglomerates and provide for the needed fast rates of dispersion and distribution of the API particulates for the dissolution, *and dissolution alone*, to proceed and be completed *during a time period where we can estimate dissolution rates.*

In the *DE* part of the torque trace curve, the torque is rising along with the temperature so the dispersion of APAP particles had to be involved. And since the dissolution was also proceeding simultaneously, this part of the curve shall be generated as the co-effect of both dispersion and dissolution of the APAP particles.

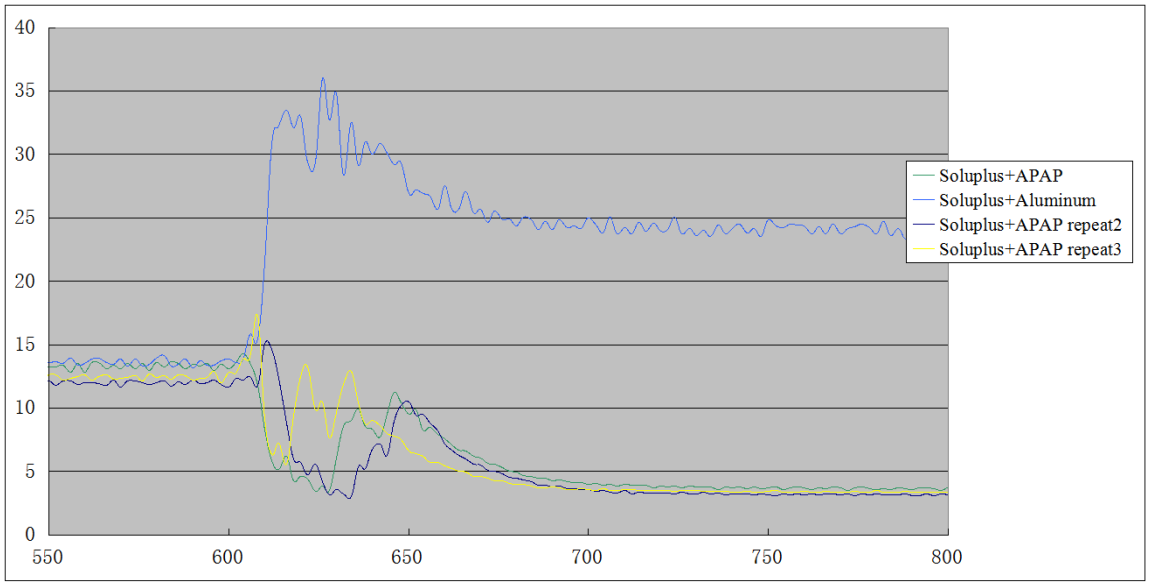

Figure 4.11 Torque traces of Soluplus upon the addition of APAP (repeat 2 times) and Aluminum (Magnified/Expanded scale)

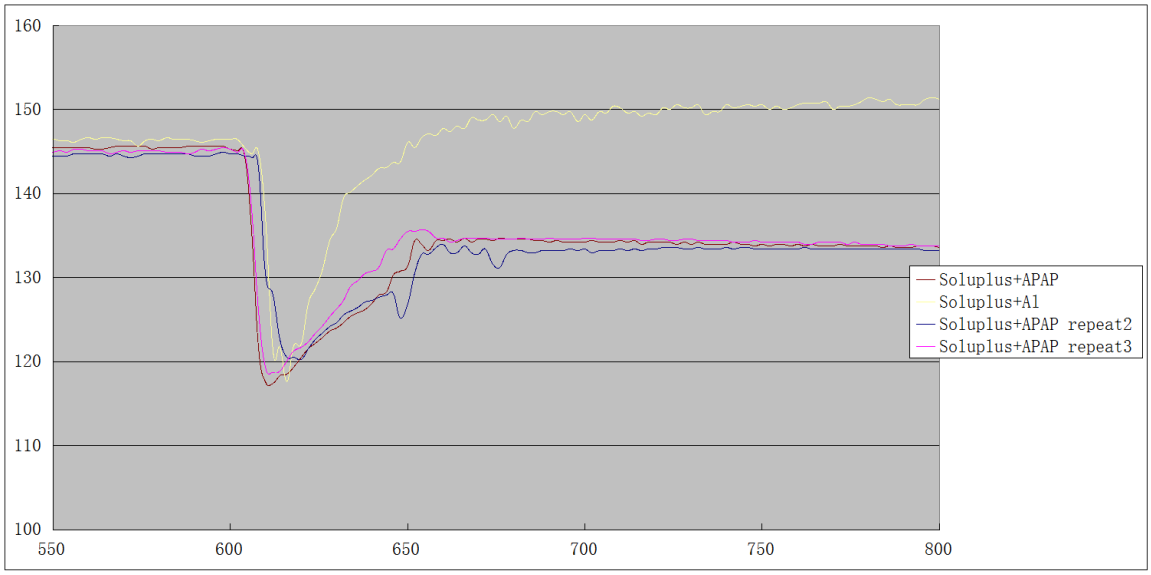

Figure 4.12 Temperature traces of Soluplus upon the addition of APAP (repeat 2 times) and Aluminum (Magnified/Expanded scale)

As we can see from the repeated experiments of Soluplus/APAP above in Figure 4.11 and 4.12, although there are some variations that can be observed at the yellow curve in Figure 4.11 (referred as Soluplus+APAP repeat3) which may be due to the random

dispersion behaviour of the APAP agglomerates in the Soluplus melt, the basic trends of the curves are as described previously.

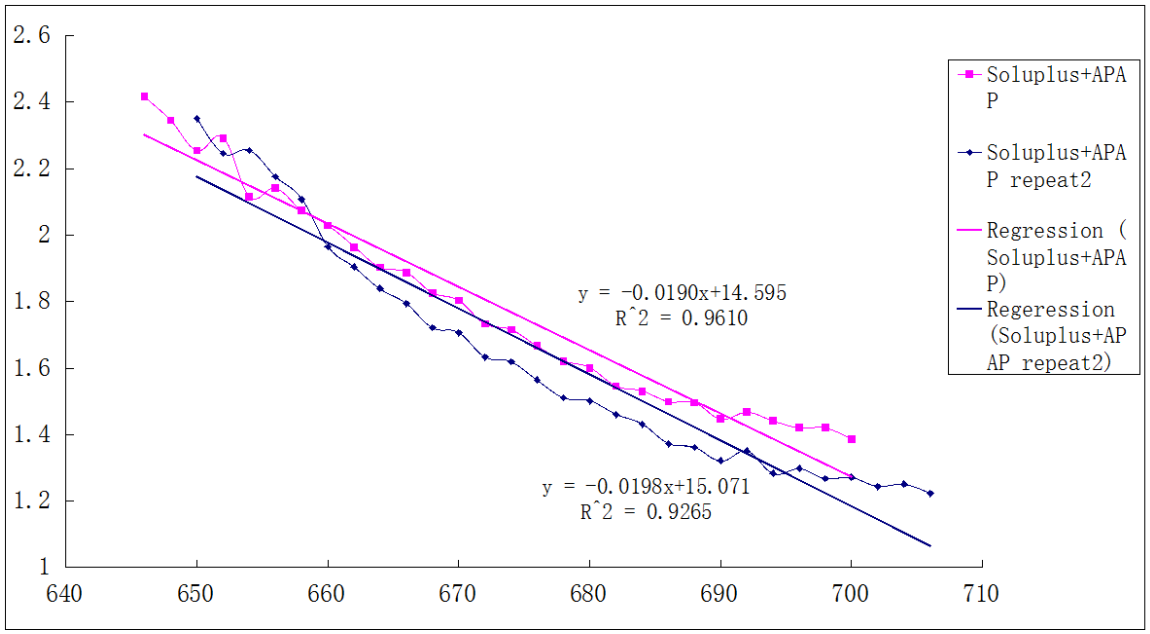

Figure 4.13 The dissolution estimation by the plot of ln M vs. Time.

We can now proceed with the *estimation of the exponential decay rate* of dissolution of the APAP in the polymer melt suspension during the time period denoted Points E and F, from approximately 646 – 700 s, when we assume that only dissolution takes place. The result is shown and analyzed in the Figure 4.13 (the pink curve referred as Soluplus+APAP). According to Figure 4.13, it appears that the torque (referred as M) is proportional to the time through the exponential relationship. So the relation of the torque of the APAP-Soluplus polymeric melt *M* and time *t* can be expressed as below:

$$M = Ne^{-Kt} \tag{4.2}$$

where *N, K* are constants. According to the figure, K=0.0190 and ln N=14.595. Because the temperature and the rotation speed are treated as constants in this time period, and the

torque is proportional to the viscosity of the polymeric melt matrix, we can presume that the amount of the undissolved APAP is proportional to the viscosity and hence have the similar relation to time as that of the torque.

Using the same method, the estimation of the decay rate of the second experiment of APAP added into Soluplus can also be proceeded (shown in Figure 4.13 as the blue curve referred as Soluplus+APAP repeat2). The time period selected here is from 650s to 706s. In this case, K=0.0198 and ln N=15.071, both are close to the data of the original curve.

The whole procedure of this interesting and complex "compounding physics" phenomena presented above in a physically reasonable cartoon representation form above shown as graph in Figure 4.10 for visualization. The APAP particles are shown in black, the molten Soluplus phase is the "white" matrix, and the "gray" background is the Soluplus/APAP solution.

CHAPTER 5

SUMMARY CONCLUSIONS AND FUTURE WORK

5.1 Summary

In this work we selected a non-dissolving, surrogate material as an attempt to de-convolute the phenomena of distribution, dispersion and dissolution of the API inside a molten polymeric matrix using a Brabender batch mixer, in order to determine the dissolution kinetics of the API. Acetaminophen (APAP) and amphiphilic polyvinyl caprolactam-polyvinyl acetate-polyethylene glycol graft copolymer (PVCap- PVAc-PEG) (Soluplus) were chosen as the model API and polymer.

During the stage of screening and choosing the appropriate surrogate, SEM and optical microscope were used in size/size distribution and morphology studies. After data collection, comparison and selection, Aluminum powder was chosen as the suitable non-dissolving surrogate. The increase in the melt viscosity of a polymer upon the addition of particulates depends not only on the particle size/size distribution but also the volume fraction, the surface tension, the specific heat capacity and the aspect ratio of the added particles. The aspect ratio can be neglected if it is below 10, which is true for both APAP and Al particles. However other properties, such as density, specific heat and surface tension are quite different for the particle types used in this work.

Because of these different values of these parameters, an investigation on the effect of different particle properties on the melt viscosity of Soluplus during melt mixing was also conducted. The experiments show that the particle size will affect the viscosity of the final surrogate/polymer melt matrix through different contacting areas. We also observed that the initial temperature of the added particles can also affect the viscosity. This is presumed to be because of the "wetting" effect leading to larger contacting surface area. From the above investigations we concluded that it is very difficult to find a "perfect" surrogate. We therefore decided to proceed with Al powder as the surrogate.

As the surrogate was selected, two batch mixer runs has been conducted to compare the torque and temperature traces of the Al or APAP added into the Soluplus melt matrix. In the comparison and analysis, the different steps of the dispersion and dissolution can be identified. In this trial, the dispersion, distribution and dissolution phases are not completely separated but we have observed and identified a period where there is basically only the dissolution of the API that takes place, enabling us to estimate dissolution rates.

The broader picture revealed in this study is vivid evidence that Pharma HME is essentially a special case of polymer compounding in which phenomena, in addition to the dissolution of the API into the polymer melt, occur at the same time and at different rates, at given processing periods.

5.2 Future Work

The chosen surrogate, Al, is considered to be imperfect because of the different thermal conductivity, heat capacity and surface tension from those of the API particles. So, further efforts can be devoted to the searching of a better surrogate that will have similar characteristics with the API. Besides, the comparison of the Al and APAP can be conducted with the similar experiment but under other different conditions like altered set temperature of the mixer or changed rotation speed, in order to have a better view of the steps of dispersion, distribution and dissolution.

It is also important to address the issue of using processing conditions and API/Excipient pairs which will yield fast particulate dispersion rates and slow dissolution rates. An example of this will be a series of lower processing temperatures.

REFERENCES

G. Terife, N. Faridi, C.G. Gogos, 2012. *SPE-ANTEC Tech. Papers*.

Z. Tadmor, C.G. Gogos, 2006. *Principles of Polymer Processing*, Wiley: Hoboken, New Jersey.

C.G. Gogos, H. Liu, P. Wang, in: Douroumis, ed., 2012. *Hot-Melt Extrusion: Pharmaceutical Applications*, Wiley: Chichester, UK.

W. Thiele, in: Ghebre-Sellassie, Martin, ed., 2003. *Pharmaceutical Extrusion Technology*, CRC Press: New York, New York.

C.G. Gogos, H. Liu, P. Wang, 2012. *Laminar Dispersive and Distributive Mixing with Dissolution and Application to Hot-melt Extrusion,* John Wiley & Sons Ltd: Chichester, UK.

M.M. Crowley, F. Zhang, M.A. Repka, S. Thumma, S.B. Upadhye, S.K. Battu, J.W. McGinity, C. Martin, 2007. *Pharmaceutical Applications of Hot-Melt Extrusion: Part I. Drug Dev. Ind. Pharm.*, 33, 909-926.

S.U. Yoo, S.L. Krill, Z. Wang, C. Telang, 2009. *Miscibility/Stability Considerations in Binary Solid Dispersion Systems Composed of Functional Excipients Towards the Design of Multi-Component Amorphous Systems.* J. Pharm. Sci., 98, 4711-4723.

C. Bruce, K.A. Fegely, A.R. Rajabi-Siahboomi, J. W. McGinity, 2007. *Crystal Growth Formation in Melt Extrudates*. Int. J. Pharm. 341: 162-172.

W. Doll, L. Konczol, L. Bevan, 1985. *Encyclopedia of Polymer Science and Engineering, 2nd edition.* 9: 745-760.

I. Ghebre-Sellassie, C. Martin, 2007. *Pharmaceutical Extrusion Technology*. Informa Healthcare, New York, New York.

H. Liu., May 2010. *Hot Melt Mixing/Extrusion and Dissolution of Drug (Indomethacin) in Acrylic Copolymer Matrices*. Ph.D. Dissertation. New Jersey Institute of Technology, Newark, NJ.

D.J. Greenhalgh, A. C. Williams, P. Timmins, P. York, 1999. *Solubility Parameters as Predictors of Miscibility in Solid Dispersions*. J. Parm. Sci. 88: 1182-1190.

A. Forster, J. Hempenstall, I. Tucker, T. Rades, 2001. *Selection of Excipients for Melt Extrusion with Two Poorly Water-soluble Drugs by Solubility Parameter Calculation and Thermal Analysis*. Int. J. Pharm. 226: 147-161.

D.Q.M. Craig, 2002. *The Mechanisms of Drug Release from Solid Dispersions in Water-soluble Polymers.* International Journal of Pharmaceutics. 231: 131-144.

P.J. Marsac, T. Li, and L.S. Taylor, 2008. *Estimation of Drug–Polymer Miscibility and Solubility in Amorphous Solid Dispersions Using Experimentally Determined Interaction Parameters*. Pharmaceutical Research 26(1): 139-151.